arXiv:1406.2575v1 [cond-mat.soft] 10 Jun 2014

Complex Rheology of Nematogenic Fluid; Connection to Elastic Turbulence

Rituparno Mandal,[1,*] Buddhapriya Chakrabarti,[2,†] Debarshini Chakraborti,[1] and Chandan Dasgupta[1,‡]

[1] *Centre for Condensed Matter Theory, Department of Physics, Indian Institute of Science, Bangalore 560012, India*
[2] *Department of Mathematical Sciences, Durham University, South Road, Durham DH1 3LE,United Kingdom.*

We numerically analyse the full non-linear hydrodynamic equations of a sheared nematic fluid under shear stress and strain rate controlled situations incorporating spatial heterogeneity in the gradient direction. For a certain range of imposed stress and strain rates, this extended dynamical system shows signatures of *spatio-temporal chaos* and *transient shear banding*. In the chaotic regime the power spectra of the order parameter stress and the total injected power shows power law behavior and the total injected power shows a non-Gaussian, skewed probability distribution, which bear striking resemblance to *elastic turbulence* phenomena observed in polymer solutions. The scaling behavior is independent of the choice of shear rate/stress control method.

PACS numbers: 47.20.-k, 47.57.Lj, 47.27.-i

Rheology of sheared wormlike micelles shows spatiotemporal chaos at very low Reynold's numbers, arising from constitutive material nonlinearities, referred to as "rheochaos"[1, 2, 7]. Similarly sheared polymeric liquids show irregular flow behavior with fluid motion excited over a large range of spatial and temporal scales. This behavior, akin to turbulent phenomena in Newtonian fluids, is termed "elastic turbulence" [8, 9, 13]. Both these phenomena show very similar statistical properties, *e.g.* power law decay in the power spectral density (PSD) of fluctuating quantities like shear rate/shear stress, depending on the controlling protocol. In addition experiments on elastic turbulence show skewness and non-Gaussianity of the probability distribution function (PDF) of total injected power [13, 16].

In this paper we bridge the connection between elastic turbulence and rheochaos by numerically analyzing the equations of nematic hydrodynamics under (a) shear rate, and (b) shear stress controlled conditions. Previous numerical studies implementing a shear rate controlled protocol with spatial heterogeneity and passive advection [5, 6] as well as incorporating velocity feedback [12] showed presence of spatiotemporal chaos. The main results of the present study can be summarized as follows: *(i)* while the temporal dynamics of the nematic order parameter of a homogeneous system with stress control [17] does not show chaos, the full hydrodynamic model incorporating spatial heterogeneity shows spatiotemporal chaos, *(ii)* the spatial and temporal power spectrum of the order parameter stress show a power law scaling with the wave vector and frequency, with identical exponents for both protocols, and *(iii)* the statistical properties of the spatio-temporally chaotic phase found in this model bear a strong similarity with those characterizing "elastic turbulence" in polymer solutions [8, 9, 13], suggesting an intriguing connection between our model system and systems which are studied in experiments on "elastic turbulence".

We have studied a phenomenological model, proposed by Hess *et al.* [10] that considers the hydrodynamic

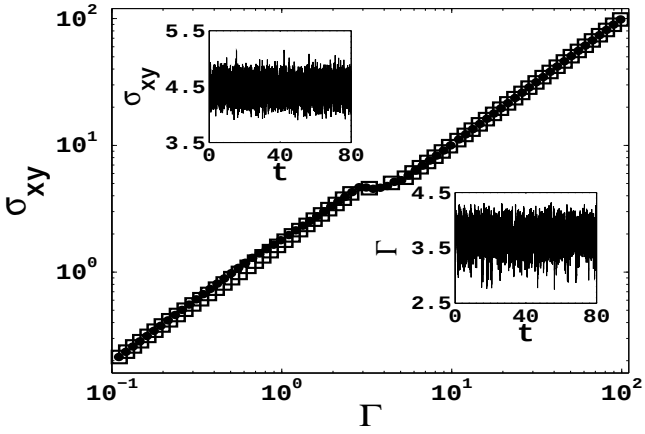

FIG. 1: Flow curve for the parameter values $\lambda_k = 1.12$, $\eta = 1.0$, in shear rate (filled circles) and shear stress (open squares) controlled simulations. Insets show (in the unstable region of the flow curve) the fluctuation in the shear stress σ_{xy} (shear rate Γ) with respect to time t (in units of 1000 computational time units), when the shear rate (shear stress) is held constant.

relaxation equation of the alignment tensor $\mathbf{Q}$ of a complex nematogenic fluid incorporating spatial heterogeneities [5, 6]. The equation of motion obeyed by the nematic alignment tensor $\mathbf{Q}$ is

$$\frac{\partial \mathbf{Q}}{\partial t} + \mathbf{u}.\boldsymbol{\nabla} \boldsymbol{Q} = \tau^{-1}\mathbf{G} + (\alpha_0 \boldsymbol{\kappa} + \alpha_1 \boldsymbol{\kappa}.\mathbf{Q})_{ST} + \mathbf{Q}.\boldsymbol{\Omega} - \boldsymbol{\Omega}.\mathbf{Q}, \tag{1}$$

where, τ is a "bare" relaxation time, α_0 and α_1 are flow alignment parameters related to molecular shapes, the subscript 'ST' denotes symmetrization and trace removal of the tensorial quantities and, and $\boldsymbol{\kappa} \equiv (1/2)[\boldsymbol{\nabla u} + (\boldsymbol{\nabla u})^T]$ and $\boldsymbol{\Omega} \equiv (1/2)\,[\boldsymbol{\nabla u} - (\boldsymbol{\nabla u})^T]$ are the shear rate and vorticity tensors respectively. The imposed flow geometry is plane Couette type with velocity $\mathbf{u} = y\Gamma\hat{\mathbf{x}} + \delta_1\hat{\mathbf{x}} + \delta_2\hat{\mathbf{z}}$ where δ_1 and δ_2 are y-dependent perturbations in the velocity profile and Γ is the shear rate. Therefore the flow is along the x axis, the z axis is

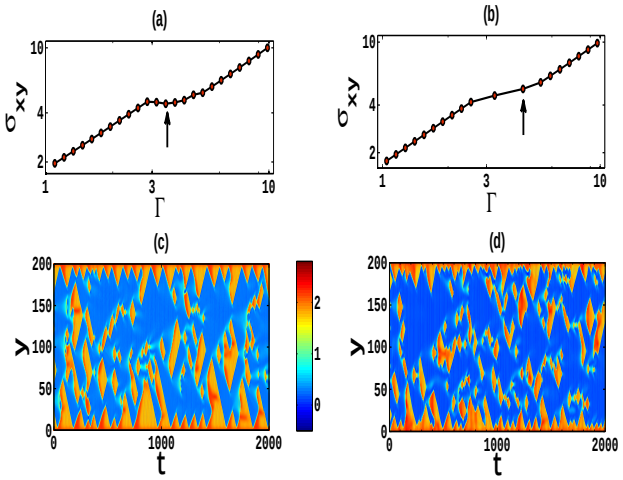

FIG. 2: (color online) Flow curve for (a) strain rate controlled and (b) shear stress controlled protocols for parameters $\lambda_k = 1.12$, $\eta = 1.0$ and corresponding space time plots for the order parameter stress σ_{xy}^{OP} (see text) (panels (c) and (d), respectively) for the unstable part of the flow curve indicated by an arrow. Same color bar has been used for both the plots in panels (c) and (d).

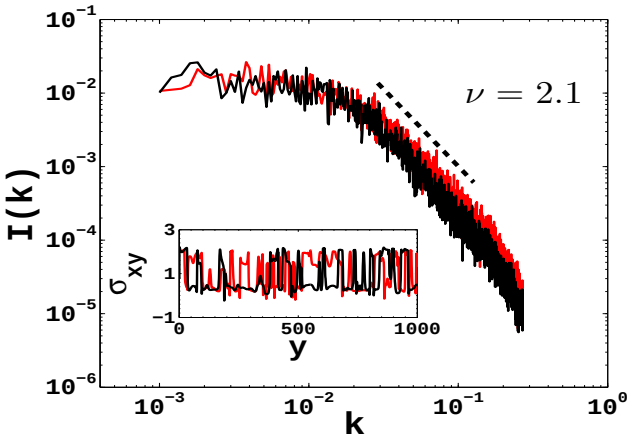

FIG. 3: (color online) Spectrum in the wave vector domain, obtained by taking the Fourier transform of the spatial profile of the order parameter stress σ_{xy}, averaged over 10 time instances (separated by a time scale longer than the correlation time) in both shear stress (black) and shear rate (red) controlled simulation for $\lambda_k = 1.12$. The dashed line is a power law fit of the form $I(k) \sim k^{-\nu}$ with $\nu = 2.1$. The inset shows the spatial variation of the order parameter stress in shear rate (red) and shear stress (black) controlled simulation at an arbitrary time instance in the steady state.

the vorticity direction and spatial variations are allowed only in the gradient direction (the y axis). Thus, we effectively have a quasi-one-dimensional hydrodynamic model for the nematic order parameter and velocity fields.
In Eq.(1), $\mathbf{G}$ is the molecular field conjugate to $\mathbf{Q}$ *i.e.* $\mathbf{G} = -\frac{\delta F[\mathbf{Q}]}{\delta \mathbf{Q}}$ where $F[\mathbf{Q}]$ is the Landau-De Gennes free energy functional,

$$F[\mathbf{Q}] = \int d^3x [\frac{A}{2}\mathbf{Q}:\mathbf{Q} - \sqrt{\frac{2}{3}}B(\mathbf{Q}\cdot\mathbf{Q}):\mathbf{Q} + \frac{C}{4}(\mathbf{Q}:\mathbf{Q})^2 + \frac{\Gamma_1}{2}\boldsymbol{\nabla Q}\vdots\boldsymbol{\nabla Q} + \frac{\Gamma_2}{2}\boldsymbol{\nabla}.\boldsymbol{Q}.\boldsymbol{\nabla}.\boldsymbol{Q}], \quad (2)$$

with phenomenological constants A, B, C controlling the free energy difference between the isotropic and nematic phases and Γ_1 and Γ_2 related to the Frank elastic constants.

The total stress $\boldsymbol{\sigma}$ in the system is the sum of bare viscous stress $\boldsymbol{\sigma}^{vis}$ and order parameter stress $\boldsymbol{\sigma}^{OP}$. The viscous stress is of the form $\boldsymbol{\sigma}^{vis} = \mu[(\boldsymbol{\nabla}\mathbf{u}) + (\boldsymbol{\nabla}\mathbf{u})^T]$ where μ is the viscosity of the nematogenic fluid and the deviatoric order parameter stress $\boldsymbol{\sigma}^{OP}$ can be written as

$$\boldsymbol{\sigma}^{OP} = -\alpha_0\mathbf{G} - \alpha_1(\mathbf{Q}.\mathbf{G})_{ST}. \quad (3)$$

We assume that the fluid is incompressible *i.e.* $\boldsymbol{\nabla}.\mathbf{u} = \mathbf{0}$ and work in the zero Reynolds number or Stokesian limit *i.e.* $\boldsymbol{\nabla}.\boldsymbol{\sigma} = \mathbf{0}$.

When spatial variations are allowed only in the gradient direction, the Stokes condition enforces $\boldsymbol{\sigma}$ to be constant in space. In the shear rate controlled case we implement this constraint by imposing

$$\mu\frac{\partial^2 u_i}{\partial y^2} = -\frac{\partial \sigma_{yi}^{OP}}{\partial y}, \quad (4)$$

where $i = x, z$ for the specific flow geometry considered. For the shear stress controlled case $\boldsymbol{\sigma}$ is constant in space and time and this restriction is incorporated by imposing

$$\mu\frac{\partial u_i}{\partial y} = \sigma_{yi}^{imp} - \sigma_{yi}^{OP}, \quad (5)$$

where $\boldsymbol{\sigma}^{\boldsymbol{imp}}$ is the imposed shear stress.

Recently Klapp *et al.* [17] have implemented a protocol to study stress controlled rheology of nematogenic fluids. In this model the instantaneous shear stress σ_{xy} is expressed in terms of a time-dependent shear rate $\Gamma(t)$ and the deviatoric stress contribution from the order parameter tensor (Eq. 3). The rate of change of the shear rate $\Gamma(t)$ with respect to time is set to be proportional to the difference between the instantaneous and imposed stresses. This ensures stress control for times $t > \tau_g$, where τ_g is a time scale over which the "control" takes effect. The controlling protocol implemented in this paper does not suffer from this limitation and (Eq. 5) ensures that the shear stress is exactly equal to the imposed value at each time instant.

The order parameter $\mathbf{Q}$ and its time evolution (Eq. 1) can be expressed in a orthonormal basis with five independent components $a_0, a_1, \ldots a_4$ [3, 5]. These equations along with Eq. 4 and Eq. 5 (depending on the controlling

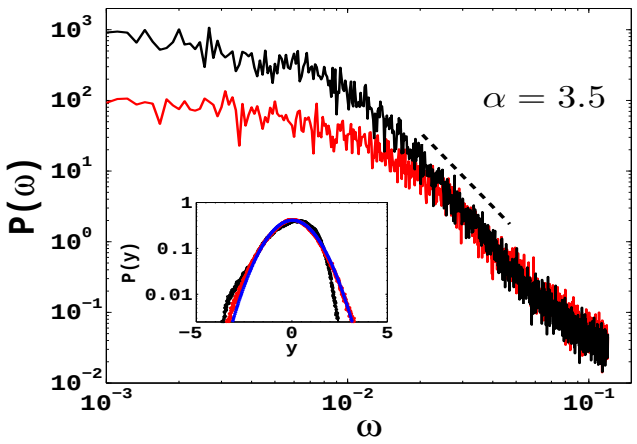

FIG. 4: (color online) Power spectral density in the frequency domain of total injected power ($p(t)$) in shear stress (black) and shear rate (red) controlled simulations for $\lambda_k = 1.12$. The dashed line shows a power law decay of the form $P(\omega) \sim \omega^{-\alpha}$ with $\alpha = 3.5$. The inset shows the probability distribution function of the normalised fluctuation (y) of the total injected power (see text) for both shear rate (red) and shear stress (black) controlled methods and the solid blue line is a gaussian fit. The probability distribution function clearly shows non-Gaussianity and negative skewness.

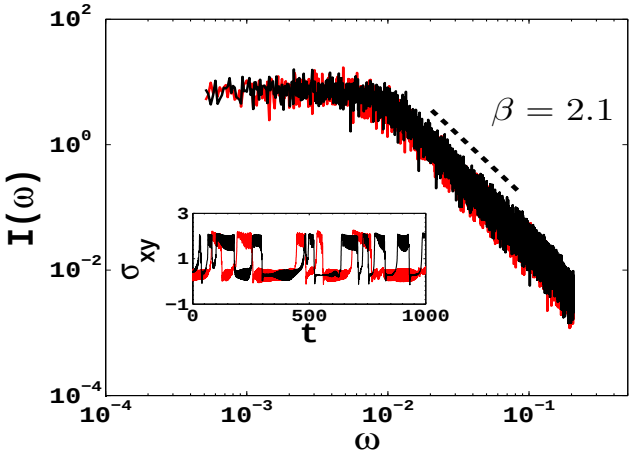

FIG. 5: (color online) Power spectral density in the frequency domain of the order parameter stress σ_{xy}, averaged over 10 space points (separated by distances greater than the correlation length), in both shear stress (black) and shear rate (red) controlled simulations for $\lambda_k = 1.12$. The dashed line shows a power law decay of the form $I(\omega) \sim \omega^{-\beta}$ with $\beta = 2.1$. The inset shows the time variation of the order parameter stress in shear rate (red) and shear stress (black) controlled simulations at a fixed space point.

protocol) provide the full hydrodynamic description of a sheared nematic fluid. We have rescaled space by the diffusion length constructed from Γ_1 and A_*, time by τ/A_* and $\mathbf{Q}$ by Q_k where $A_* = \frac{2B^2}{9C}$ and Q_k is the magnitude of $\mathbf{Q}$ at the transition temperature. The equations of motion of the nematic director have several independent parameters: A, Γ, Γ_2/Γ_1, α_1, λ_k and η where $\lambda_k = \sqrt{\frac{2}{3}}\frac{\alpha_0}{Q_k}$ and $\eta = \mu/(\alpha_0 \tau Q_k)$. The results presented here are for $\Gamma_2/\Gamma_1 = 1$, $A = 0$, $\alpha_1 = 0$ and $\eta = 1$. We have carefully verified that our results are insensitive to small changes in these parameters. We set $\sigma_{yz}^{imp} = 0$ in the stress controlled case. Thus we have two independent parameters: the imposed shear stress σ_{xy}^{imp} or the shear rate (Γ) and the tumbling parameter (λ_k).

The equation for the time evolution of the director field, Eq. 1 expressed in terms of the components $a_0, a_1 \ldots a_4$, is solved numerically. A symmetrized finite difference scheme is used to compute the spatial derivatives while the equations are integrated forward in time using a fourth-order Runge-Kutta scheme with a fixed time-step $\Delta t = 0.001$. The fluid velocity is calculated using Eq. 4 or Eq. 5 at each time step and fed back in Eq. 1 to compute the instantaneous order parameter profile. The fluid velocity for the shear rate controlled case is obtained by expressing Eq. 4 as a matrix equation and performing a matrix inversion using a LAPACK subroutine.

Fixed boundary conditions are implemented for the velocity field $\mathbf{u}$ and the order parameter field $\mathbf{Q}$, with the $\mathbf{Q}$ tensor corresponding to the nematic director being along $\hat{z}$ at the walls (*i.e.* at $y = 0$ and $y = L$). We have checked that the behavior in the bulk does not depend on the alignment of the nematic director at the boundaries. The boundary conditions for the velocity field are $\delta_1 = \delta_2 = 0$ at both the boundaries (which ensures steady shear) for the shear rate controlled case while $\delta_1 = \delta_2 = 0$ only at the static boundary for the shear stress controlled situation. We have studied system sizes varying between $L = 100$ to 10000 with grid size $\Delta x = 0.1$. We have verified that smaller values of the grid size or the integration time step do not change the results qualitatively.

By keeping λ_k fixed between 0.9 to 1.15 and varying the shear rate Γ or the shear stress σ_{xy}^{imp}, we find three distinct steady states or "phases" (i) *periodic*, (ii) *spatiotemporally chaotic*, (see Fig. 2) and (iii) *aligned*. In the shear rate controlled case, the flow curve (see Fig. 1) shows non-monotonic behavior in a small range of Γ values, whereas the shear stress controlled flow curve shows discontinuous jumps in the shear rate when shear stress is changed by only a little amount. On closer inspection, this region reveals the existence of a spatio-temporally chaotic phase. A detailed investigation of the order parameter stress and velocity profile in the spatiotemporally chaotic phase shows transient shear banding with randomly nucleating domains of low and high stress (see Figs. 2(c) and (d) and 3 inset) that evolve as a function of time revealing bistable behavior (see Fig. 5 inset) for both controlling protocols.

We have analyzed the statistical properties of the space and time series of the order parameter stress (Eq. 3) and

the time series of the total injected power $p(t) = \Gamma\sigma_{xy}$. Fig. 3 shows the power spectrum of the spatial variation of the order parameter stress as a function of the wave number k and a power law scaling behavior $I(k) \sim k^{-\nu}$ with $\nu \approx 2.1$, which is observed for both control protocols in the spatiotemporally chaotic phase. Fig. 5 shows the power spectrum of the order parameter stress in the frequency domain ω in the spatiotemporally chaotic phase. Here also a power law scaling behavior is observed, *i.e.* $I(\omega) \sim \omega^{-\beta}$ with $\beta \approx 2.1$ for both control protocols. Experiments measuring reflected light intensity (which captures the director configuration and thereby is an indirect measure of the order parameter stress) at a given time instant as a function of space or at a fixed space point as a function of time, show scaling behavior with similar exponents [8, 9]. The total injected power $p(t)$ is a fluctuating global quantity whose power spectral density shows a power law decay, $P(\omega) \sim \omega^{-\alpha}$ with the exponent $\alpha \approx 3.5$ for both control protocols as shown in Fig. 4. This satisfies the Fuoxon-Lebedev criterion [15] ($|\alpha| > 3$), which is known to be satisfied in experiments on elastic turbulence [8, 9, 13]. The probability distribution of the normalized fluctuation of the total injected power, defined as $y = \frac{p-\langle p\rangle}{\sigma_p}$, where $\langle p\rangle$ is the mean value and σ_p the standard deviation of the instantaneous injected power $p(t)$, shows negative skewness and non-Gaussian behavior (see Fig. 4 inset). Similar behavior is observed in experiments on elastic turbulence in polymer solutions [8, 13, 16].

We have also studied the Lyapunov spectrum [11] of the order parameter stress time series data for this system. Fig. 6 shows that the number of positive Lyapunov exponents $N_{\lambda+}$ as well as the maximum Lyapunov exponent λ_{max} (see inset) increases as a function of subsystem size N_s [19] indicating that the observed fluctuations in the time series data is a signature of underlying spatiotemporally chaotic behavior.

In conclusion we have numerically analysed the fully non-linear hydrodynamic equations of a sheared nematic fluid under shear stress and strain rate controlled situations incorporating spatial heterogeneity in the gradient direction. We find that the director fluctuations in the unstable region of the flow curve for both controlling protocols show signatures of spatiotemporally chaotic behavior. A detailed analysis of the statistical properties of the fluctuating data train shows striking resemblance with those observed in elastic turbulence phenomena in sheared polymer solutions. Though several approximations have been used in this study (*e.g* Stokes limit, incompressibility condition, spatial variation only in the gradient direction *etc.*) this resemblance is exciting and it paves the way of extending theoretical work carried out in the field of liquid-crystals to analyse experimental data on elastic turbulence. In future, we hope to carry out numerical investigations on a more realistic model considering spatial heterogeneities also in the vorticity direction.

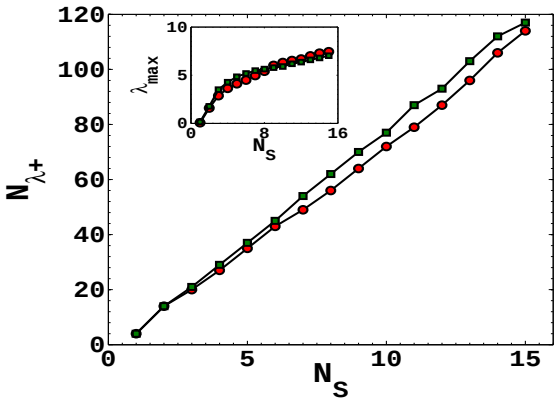

FIG. 6: (color online) Number of positive Lyapunov exponents as a function of sub-system size N_s for shear rate (red) and shear stress (green) controlled methods for $\lambda_k = 1.12$. The inset shows the maximum Lyapunov exponent as a function of sub-system size N_s for shear rate (red) and shear stress (green) controlled simulations.

We hope that such a study will capture the interfacial gradient banding instability seen in experiments. Further we wish to extend the model to study Navier-Stokes equation in two and three dimensions coupled with the equations for the order parameter. We hope that our work will spark interest among experimentalists to probe the connection between rheochaos in nematic fluid and elastic turbulence in polymers further.

We thank A. K. Sood and Ananyo Maitra for very useful discussions. R. M. acknowledges financial support from CSIR, India. C. D. G. acknowledges financial support from DST, India. B. C. acknowledges support from Durham University and IISc Bangalore for hospitality.

* Email: rituparno@physics.iisc.ernet.in
† Email: buddhapriya.chakrabarti@durham.ac.uk
‡ Email: cdgupta@physics.iisc.ernet.in

[1] R. Bandyopadhyay, G. Basappa, A. K. Sood, Phys. Rev. Lett, **84** 2022, (2000).
[2] R. Ganapathy and A.K. Sood, Phys. Rev. Lett. **96**, 108301 (2006).
[3] G. Rienäcker, M. Kroger, and S. Hess, Phys. Rev. E **66**, 040702(R) (2002).
[4] G. Rienäcker, M. Kroger, and S. Hess, Physica A **315**, 537 (2002).
[5] B. Chakrabarti, M. Das, C. Dasgupta, S. Ramaswamy and A.K. Sood, Phys. Rev. Lett. **92**, 055501 (2004).
[6] M. Das, B. Chakrabarti, C. Dasgupta, S. Ramaswamy and A.K. Sood, Phys. Rev. E **71**, 021707 (2005).
[7] R. Ganapathy, S. Majumdar and A.K. Sood, Phys. Rev. E **78**, 021504 (2008).
[8] S. Majumdar and A.K. Sood, Phys. Rev. E. **84**, 015302 (2011).
[9] M. A. Fardin *et al.* Phys. Rev. Lett **104**, 178303 (2010).
[10] S. Hess, Z. Naturforsch. **30a**, 728 (1975), Z. Naturforsch.

31a, 1034 (1976).
[11] R. Hegger, H. Kantz and T. Schreiber, CHAOS **9**, 413 (1999).
[12] D. Chakraborty, C. Dasgupta and A.K. Sood, Phys. Rev. E **82**, 065301 (2010).
[13] A. Groisman and V. Steinberg, Nature (London) **405**, 53 (2000), V. Steinberg *et al.* Phys. Rev. Lett. **102**, 124503 (2009), *ibid.* **96**, 214502 (2006).
[14] D. Chakraborty, PhD. Thesis, Series/Report Number: G24864, Indian Institute of Science
[15] A. Fouxon, V. Lebedev, Phys. Fluids **15**, 2060 (2003).
[16] J. F. Pinton, P. C. W. Holdsworth, and R. Labbe, Phys. Rev. E **60**,2452(R) (1999), and references cited therein.
[17] Sabine H. L. Klapp and Siegfried Hess, Phys. Rev. E **81**, 051711 (2010).
[18] S. M. Fielding, Phys. Rev. Lett. **95**, 134501 (2005).
[19] R. Hegger, H. Kantz, and T. Schreiber, Practical implementation of nonlinear time series methods: The TISEAN package, CHAOS **9**, 413 (1999)